The QRS-Integral of an Electrogram as an Indicator of the Subsequent Local Activation Duration

A van Oosterom, V Jacquemet

Dept. of Cardiology, University of Lausanne, Lausanne, Vaud, Switzerland

Abstract

In clinical electrophysiological studies the information extracted from measured electrograms is mainly limited to the timing of local depolarization. We investigated the relation between the activation recovery interval (ARI) and electrogram waveform morphology in 3D structures. Of the various features extracted from simulated electrograms on the surface bounding the myocardium the integrals over a time interval around local depolarization showed the highest correlation with nearby ARI values.

1. Introduction

The dominant part of an electrogram measured close to the myocardial surface with respect to some distant reference electrode usually has some kind of an RS waveform morphology. The timing of the fastest down slope in the observed signal is a reliable indicator of local activation. Following that signal component a generally much smaller and much slower one is found that in some way represents the ongoing repolarization processes throughout the myocardium. Here the link with the timing of local repolarization, quantified by whatever feature, is far less direct.

The current interest in repolarization phenomena and their quantification by means of some measure of action potential duration, in particular with possible inferences for the diagnosis of atrial fibrillation (AF), forms the motivation for this study.

The analysis of electrograms simulated by means of our realistic, biophysical atrial model suggested a relationship between the local action potential duration and morphology of the RS spike. In an ongoing study this relationship is explored. In particular the geometrical factors of the curvature of the myocardial surface and/or of the wave front of local depolarization are investigated. In order to rule out other confounding effects, the study is based on a homogeneous representation of the myocardial tissue in which all active units that generate propagating activity have identical intrinsic parameters. Next to the realistic atrial model, the study employs more simple geometrical configurations to facilitate the quantification of curvature. This report describes some preliminary results.

2. Methods

Simulated propagation

Activation-recovery processes were initiated by stimuli applied to ensembles of coupled nonlinear differential equations having identical intrinsic parameters. The electrical propagation of the cardiac impulse was simulated using a reaction-diffusion system (monodomain formulation) based on the detailed ionic model of the cell membrane described by Courtemanche *et al.* [1,2]. The grid space of the cubical mesh coupling the active units was 0.3 mm. The velocity of the propagation set up in the systems was of the order of 0.75 m/s. The simulated TMPs were specified for single beats at 1 ms sampling intervals over 500 ms. The pacing rate was 2 beats/s.

Geometries

Three different types of geometries were involved in the study.

A. A thick-walled three dimensional biophysical model of the atria based on magnetic resonance images, comprising about 800,000 units [2]. The stimulus was delivered at the natural location of the sino-atrial node. The triangulated version of this surface comprises nver=1297 nodes.

B. A spherical shell with outer radius of 2 cm, wall thickness: 2 mm, comprising 330,000 units. The stimulus was delivered at either the 'North Pole': N_stim, the North and South pole simultaneously: NS_stim, the 'West' pole: W_stim and North and West simultaneously: NW_stim; nver=1284.

C. A thick walled diabolo-shaped geometry with axial symmetry around the z-axis, in which the outer contour was described by the radius $r(z)=a_0-a_3\cos(cz)$, with a_0=2 cm, a_3 =0.3a_0 and $c = 3\pi/(2a_0)$,

comprising 480,000 units; nver=1266. The inner surface was created at a fixed 2 mm distance from the outer wall. The stimuli were applied in the same locations as specified for geometry B.

Geometry A. has the complexity expected in a clinical situation. Geometry B has a uniform curvature that only marginally differs between its inner and outer bounds. Geometry C has the wide range of curvature values desired for this study. All stimuli were applied to the outer (epicardial) surface. For all of these geometries, the nodes were evenly distributed over the surface.

Source model

The source description used is the instantaneous distribution of transmembrane potentials (TMPs) of the myocytes at the heart surface S_h, which is taken to be the surface bounding the myocardium, *i.e.,* the closed surface bounding outer surface (epicardium) and inner surface (endocardium) of the geometries A-C. The time course of the TMP at a specific location, x, on this surface is the source strength of the unit nearest to this node, denoted as $S(x,t)$. This represents the source description derived from the Equivalent Double Layer (EDL) model of the electric sources of cardiac myocytes [3,4].

The effect of these sources as potentials $\Phi(y,x)$ observed at arbitrary field points, y, is governed by the passive volume conduction effects of the tissues surrounding the active tissue. These can be expressed by a transfer function $A(y,x)$, which permits the genesis of potentials $\Phi(y,t)$ outside the myocardium to be written as

$$\Phi(y,t) = \int_{S_h} A(y,x)\, S(x,t)\, \mathrm{d}S_h \,. \qquad (1)$$

The function $A(y,x)$ needs to be specified for the particular volume conductor configuration involved. In the current application an infinite exterior medium is assumed to have a uniform conductivity. In this situation, the function $A(y,x)$ expresses the solid angles subtended by elements $\mathrm{d}S_h$ at observation points on surface S_h . The singularities of the diagonal elements of the matrix were dealt with by means of the auto solid angle concept.

Extracted features

The features extracted from the simulated transmembrane potentials of the individual units are the timing of depolarization, δ, taken to be the time of the maximal up slope of the simulated TMP and the timing of repolarization , ρ, taken to be the time of maximal down slope (inflexion point) during repolarization. The difference $\alpha=\rho-\delta$, the activation recovery interval (ARI), is used for specifying the duration of the repolarization process. Its value is more robust than other markers of action potential duration such as APD_{90}, and ,more importantly, has a direct link with the refractory period of the action potentials [5].

The curvature values of the surface bounding the units (myocardium) are the mean curvatures derived from the local principal radii.

The integrals IQRS over time of the simulated elctrograms were computed from the simulated data by using standard numerical methods.

An asymmetry index, AI, was used to specify gross electrogram morphology during the RS period. This is defined as

$$AI = \frac{|R| - |S|}{|R| + |S|}, \qquad (2)$$

as was used in [6] as well as in [7], where it was called the RS difference. The absolute values |R| and |S| denote the amplitudes of the R waves and the S waves of the electrograms, respectively.

3. Results

Geometry A: atrial model

The waveforms of TMPs and the isochronal maps of δ (timing depolarization) and of ρ (timing repolarization, were in agreement with data known from invasive electrophysiology. Following a single stimulus at the location of the SA node, the morphology of the electrograms progressed from rS (at the stimulus site), via RS half way, to Rs near the latest activated units. The α (ARI) values decreased from about 170 ms at the stimulus site, down to about 150 ms at the nodes that were activated last. Simulated P waves based on these TMPs are shown in [4].

In Figure 1 a scatter plot is presented of the $\alpha=\rho-\delta$ (the ARI values) and the depolarization moments δ computed at all 1297 nodes of the atrial geometry (geometry A). The linear regression line shown has a slope of -0.1. The linear correlation coefficient is -0.74. The heavy line represents a moving average of the data, using a window of 4 ms. The scatter plot may have suggested a linear relationship between the data, supported by 'highly significant' value of the correlation coefficient. However, the moving average clearly shows that such a linear description would obscure the true nature of the relationship. The current study aims at identifying global factors that explain the relationship. Recall that uniform, intrinsic parameters were assigned to all units and so the explanation must come from other factors.

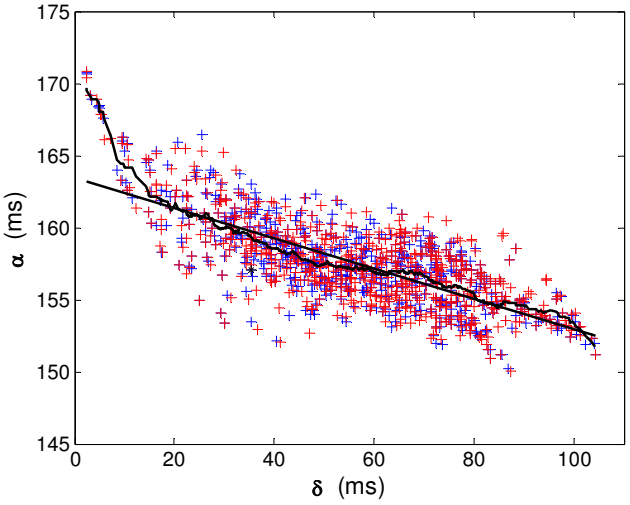

Figure 1. Scatter plot of the values δ and α at all nodes of the atrial geometry. Solid line: linear regression of α as a function of δ. Solid curve: average of the data over a window of 4 ms sliding over the δ axis. Red symbols denote endocardial nodes, blue the epicardial nodes.

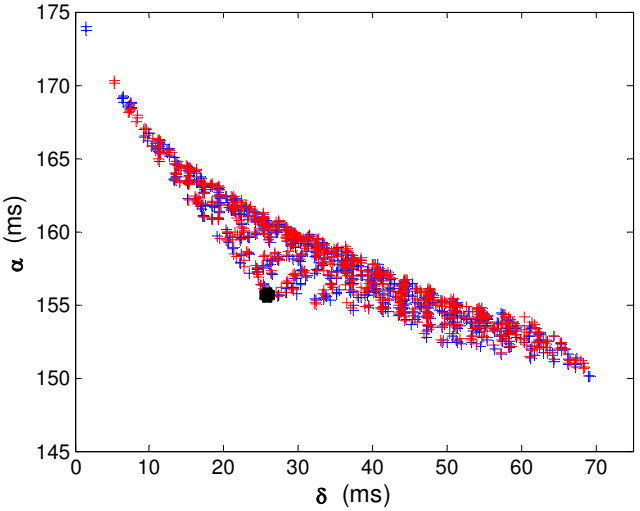

Figure 2. Scatter plot of the values δ and α at all nodes of the spherical shell resulting from the dual stimuli: NW_stim. The black dot identifies the node where the wave fronts initiated at the N-pole and the W-pole collided.

Geometry B: spherical shell

When stimulated from a single node (*e.g.* , the N_stim) the isochrones of the activation times spread out like the circles of equal latitude on a globe. The observed range of depolarization times δ was 1--89 ms, that of the α values 148--173 ms

The scatter plot of the δ and α values revealed a slide-shaped curve similar to the solid curve in Figure 1. However, here the basic data directly, *i.e.* without computing the moving average, clearly revealed the slide shape. The deviations around the curve were about 1 ms.

A more complex pattern was observed in the situation following NW_stim. The α(δ) results are shown in Figure 2. The deviations from the mean were substantial and non-random. The ranges for the δ and α values were 1--69 and 150--174 ms, respectively. The two wave fronts that started at the N-pole and the W-pole merged at 25 ms at the node identified in Figure 2 by the heavy dot. The latest point activated was at the diametrically opposed location.

Geometry C: diabolo-shaped shell

Following the N_stim, once more a narrow band around a down-sloping α(δ) curve was observed. Here the more complex geometry of the diabolo-shaped shell introduced some additional undulations of the curve at moments where the wave front passed major changes in the mean curvature of the bounding surface of the diabolo.

The ranges of δ and α values were 1--111 and 146--173 ms, respectively.

Following the NW_stim the ranges of δ and α values were 1--83 and 148--174 ms. As for geometry B, the band around a down sloping α (δ) curve was substantially wider than following the N_stim. The deviations from the main curve first increased towards lower α values, as in Figure 2. For higher values of δ the majority of the deviations shifted toward α values above the main curve. The width of the band around the final part of the curve tapered down to zero. The depolarization sequence following NW_stim is shown in Figure 3.

QRS integrals

The IQRS values of the electrograms at all nodes, for all three geometries and for all stimulus variants, were computed. A selected number of examples drawn from the NW_stim set are presented in Figure 4. Their node locations are indicated in Figure 3. Selected were: nodes N and W, the stimulus sites, nodes A and B, nodes that were activated almost simultaneously yet clearly having different α values, node S, the South pole and node F, the node that showed the final depolarization.

In all cases high, negative, linear correlation coefficients (CCs) were found between the IQRS values and the corresponding α values. For the diabolo-shaped geometry the CCs were: N_stim: -0.92; W_stim -0.92; NS_stim: -0.97; NW_stim: -0.94.

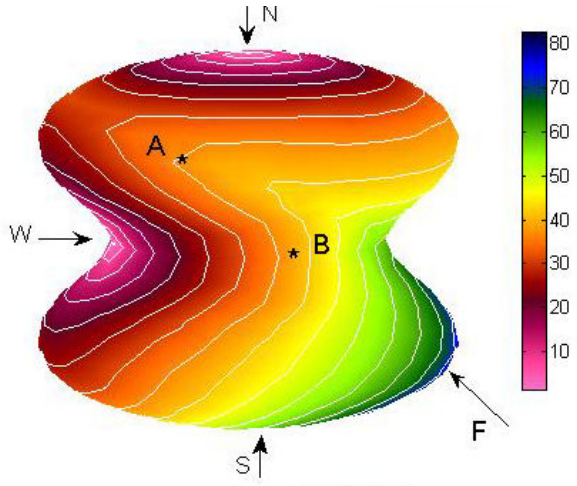

Figure 3. Isochrone map on the outer surface of the diabole-shaped shell; isochrones drawn at 5 ms intervals. The activation was initiated at poles N and W. Electrograms at locations N,W,A,B,S and F are shown in Figure 4. Note the opposite depolarization wave front curvatures at locations A and B near the same isochrone.

4. Discussion and conclusions

In spite of the uniform intrinsic properties of the units simulating the dynamics of membrane processes and their uniform coupling, the observed relationship between the δ and α values proved to be complex. The deviations of the α values from the mean α(δ) curve were positive wherever the wave front curved toward the arrow head of the vector of local propagation (*e.g.*, at node A in Figure 3). Conversely, if the wave front curved away (node B) the deviations were negative.

The extremes of the slope of the α(δ) curve were observed at the location where depolarization ended. The shape found for the major, mean down-sloping curve remains to be clarified.

The QRS integrals of the electrograms showed a surprisingly high negative CC with the ARI values for all cases studied. This corresponds to the observation that Q wave morphology of the electrograms was found at the nodes where activation started, Rs morphology wherever propagation ended or where wave fronts merged, with intermediate values in between (Figure 4.). The absolute values of the CC values of the asymmetry index, *AI*, applied to the same data were about 12 % lower, suggesting that, next to waveform amplitudes, additional waveform features may be exploited.

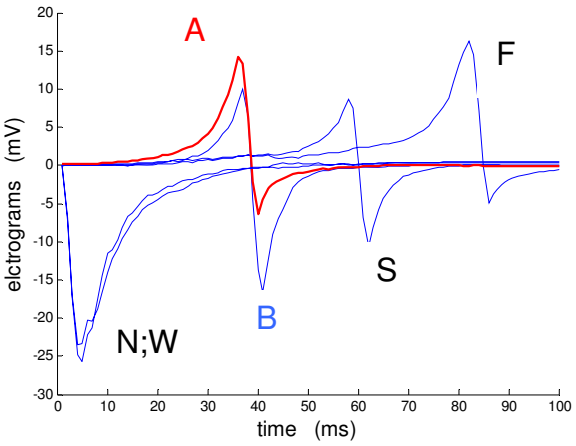

Figure 4. Electrograms (from left to right) at locations N,W,A,B,S and F as indicated in Figure 3. The heavy red line depicts the electrogram at location B.

References

[1] Courtemanche M, Ramirez RJ, Nattel S. Ionic mechanisms underlying human atrial action potential properties: insights from a mathematical model. Am J Physiol. 1998;275:301-21.

[2] Jacquemet V, van Oosterom A, Vesin JM, Kappenberger L. A biophysical model approach supporting the analysis of electrocardiograms during atrial fibrillation. IEEE Eng Med Biol Mag. 2006;In press.

[3] Geselowitz DB. On the Theory of the Electrocardiogram. Proc IEEE. 1989;77/6:857-76.

[4] van Oosterom A, Jacquemet V. Genesis of the P wave: atrial signals as generated by the equivalent double layer source model. Europace. 2005;7(Suppl 2):S21-S9.

[5] Haws CW, Lux RL. Correlation Between In Vivo Transmambrane Action Potential Durations and Activation-Recovery Intervals From Electrograms. Circulation. 1990;81/1:281-8.

[6] Jacquemet V, Virag N, Ihara Z, Dang L, Blanc O, Zozor S, et al. Study of unipolar electrogram morphology in a computer model of atrial fibrillation. J Cardiovasc Electrophysiol. 2003 Oct;14(10 Suppl):S172-9.

[7] Houben RPM, de Groot NMS, Smeets JLRM, Becker AE, Lindemans FW, Allessie MA. S-wave predominance of epicardial electrograms during atrial fibrillation; Indirect evidence for a role of the thin subepicardial layer. Heart Rhythm. 2004;1:639-47

Address for correspondence

A. van Oosterom
E-mail: adriaan.vanoosterom@epfl.ch
EPFL-STI-ITS-LTS1; ELD 241 (Bâtiment ELD); Station 11
CH 1015 Lausanne; Switzerland.